

Magnetic Circular Dichroism of the R Center in KCl^\dagger

WILLIAM BURKE*

Department of Physics and Materials Research Laboratory, University of Illinois, Urbana, Illinois

(Received 19 February 1968)

The R_2 and R_1 transitions of the R center in KCl have been studied using the technique of circular dichroism. The method of moments has been applied to analyze the effect of the magnetic field on the ground- and excited-state degeneracies. This analysis has given the magnetic parameters of the initial and final states of these transitions and provides an estimate of the ground-state orbital reduction factor due to Jahn-Teller distortions. Values for the energy of vibrational quanta of A_1 and E symmetry were determined for KCl , LiF , and $NaCl$ from the R_2 broad-band dichroism.

I. INTRODUCTION

RECENT optical¹⁻³ and electron-spin-resonance experiments^{4,5} on the R center in alkali halides have confirmed the Van Doorn model⁶ of this defect: three F centers in an equilateral triangle configuration in a (111) plane.⁷ This model possesses a $[111]$ axis of symmetry and belongs to the symmetry group C_{3h} . Silsbee's results have shown that the ground state is of 2E symmetry, that the R_2 and R_1 optical absorption bands are electric dipole transitions to final states of 2A_2 and 2E symmetry, respectively, and that to a good approximation the semicontinuum site symmetry D_{3h} is valid. Hirschfelder⁸ has calculated the low-lying energy levels for the triatomic hydrogen molecule which is formally the same as the R center in D_{3h} symmetry and has found the ground state to be a Kramers doublet of E symmetry. The spin quartet ground state for the three electrons lies higher in energy (~ 0.3 eV in KCl) and has been investigated extensively by Seidel *et al.*⁴

The orbital degeneracy of the ground state implies the possibility that the system can undergo a Jahn-Teller distortion.^{9,10} Longuet-Higgins, Opik, Pryce, and Sack (LHOPS)¹¹ have considered this problem, i.e., a doubly degenerate mode of vibration interacting with a doubly degenerate state and have calculated the eigenvalues and eigenvectors for different strengths of the first-order Jahn-Teller coupling k . The effect of this perturbation on the ground state is to couple the elec-

tronic and vibrational states and, in the notation of LHOPS, to lower the energy of the lowest vibronic level by $\frac{1}{2}k^2$. On the configuration coordinate diagram for the E modes of vibration Q_{2a} and Q_{2b} with the coordinates $Q_{2a}=r \cos\phi$ and $Q_{2b}=r \sin\phi$, the system will move in a trough of radius k . The vibronic wave functions for this system have been given by Silsbee^{1,5} from the LHOPS calculation. In this dynamic regime nonsymmetric random strains present in the crystal can lift the ground-state degeneracy. This latter effect contributes to the inhomogeneous broadening of the zero-phonon line of the R_2 band.

In this paper we present the results of a study of the effects of an applied magnetic field on the R_2 and R_1 transitions of the R center. These effects provide a measure of the orbital angular momentum and spin-orbit coupling in the ground and excited states of the R center and an estimate of the strength of the Jahn-Teller coupling constant in the ground state. Previous magneto-optic experiments include an earlier report of this work,¹² the work of Duval *et al.*,¹³ of Kuwabara,¹⁴ and a report of Shepherd.¹⁵ The results of these experiments and the work of Krupka and Silsbee⁵ will be compared later in the paper.

The remainder of this paper is divided into seven sections. Section II contains a general discussion of the effect of a magnetic field on the R center and its absorption bands. In Sec. III, the experimental apparatus is described. In Sec. IV, the method of moments is applied to the problem of a degenerate ground state. In Secs. V and VI, the method of moments is applied specifically to the R_2 and R_1 transitions and compared with the experimental results. Section VII contains the conclusions of this study.

II. GENERAL DISCUSSION

Henry, Schnatterly, and Slichter (HSS)¹⁶ have shown that the analysis of the moments of an optical absorp-

[†] This research was supported in part by the U. S. Atomic Energy Commission under Contract No. AT(11-1)-1198.

* National Science Foundation Postdoctoral Fellow. Present address: RCA Laboratories, Princeton, N. J.

¹ R. H. Silsbee, *Phys. Rev.* **138**, A180 (1965).

² F. Lanzl and W. Von Der Osten, *Phys. Letters* **15**, 208 (1965).

³ C. B. Pierce, *Phys. Rev.* **148**, 797 (1966).

⁴ H. Seidel, M. Schwoerer, and D. Schmid, *Z. Physik* **182**, 398 (1965).

⁵ D. C. Krupka and R. H. Silsbee, *Phys. Rev.* **152**, 816 (1966).

⁶ C. Z. Van Doorn, *Philips Res. Rept. Suppl.* **4** (1962).

⁷ For a review of earlier work in this field see W. D. Compton and H. Rabin, in *Solid State Physics*, edited by F. Seitz and D. Turnbull (Academic Press Inc., New York, 1964), Vol. 16, p. 121.

⁸ J. O. Hirschfelder, *J. Chem. Phys.* **6**, 795 (1938).

⁹ H. A. Jahn and E. Teller, *Proc. Roy. Soc. (London)* **A161**, 220 (1937).

¹⁰ For a review of Jahn-Teller effects in solids, see M. D. Sturge, in *Solid State Physics*, edited by F. Seitz and D. Turnbull (Academic Press Inc., New York, 1967), Vol. 20, p. 91.

¹¹ H. C. Longuet-Higgins, U. Opik, M. H. L. Pryce, and R. A. Sack, *Proc. Roy. Soc. (London)* **244**, 1 (1958).

¹² W. J. Burke, S. E. Schnatterly, and W. D. Compton, *Bull. Am. Phys. Soc.* **11**, 245 (1966).

¹³ P. Duval, J. Gareyte, and Y. Merle D'Aubigne, *Phys. Letters* **22**, 67 (1966).

¹⁴ G. Kuwabara (private communication to W. D. Compton).

¹⁵ I. W. Shepherd, *Phys. Rev.* **165**, 985 (1968).

¹⁶ C. H. Henry, S. E. Schnatterly, and C. P. Slichter, *Phys. Rev.* **137**, A583 (1965).

tion band and their changes due to external perturbations is a highly useful technique for the study of transitions involving degenerate final states. This method of analysis is necessary since the perturbation of these states due to the electron lattice interaction is generally one or two orders of magnitude larger than the perturbation arising from the applied fields. This general statement is also true even in the case of the zero phonon line of the R_2 band for the reasons cited in Sec. I. The analysis of magnetic perturbations of the R center is complicated, however, by the fact that for the R_2 transition it is the initial state that is degenerate and for the R_1 transition both the initial and final states are degenerate.

The lowest vibronic level of the E symmetry ground state of the R center can be described by Silsbee's wave functions $\Psi_{x,1,1/2}$ and $\Psi_{y,1,1/2}$. The quantum numbers 1 and $\frac{1}{2}$ describe the lowest radial excitation across the trough and the lowest angular excitation around the trough of the potential energy curve shown in Fig. 1, respectively. The degeneracy of this pair of vibronic states can be lifted by random strains of E symmetry.

Figure 2(a) shows the ground state in the absence of random strains of E symmetry and with a positive spin-orbit splitting present. The subscripts 1, $\frac{1}{2}$ on the wave functions $\Psi_{i,1,1/2}$ (where the subscript $i=x$ or y) have been omitted in Fig. 2 for clarity. The electron spin orientation is given by the arrows. The application of an external magnetic field lifts the Kramers degeneracy and the degeneracy of the orbital angular momentum eigenstates $\frac{1}{2}\sqrt{2}$ ($\Psi_{x,1,1/2} \pm i\Psi_{y,1,1/2}$). The orbital matrix element is

$$g_R = |\langle \Psi_{y,1,1/2} | L_z | \Psi_{x,1,1/2} \rangle|$$

$$= |\langle \mathcal{E}_y | L_z | \mathcal{E}_x \rangle \int r dr U_{1,1/2}(-r) U_{1,1/2}(+r)|, \quad (1)$$

since L_z operates only on the electronic wave function. The orbital matrix element is reduced by the value of the vibrational-overlap integral. Child and Longuet-Higgins¹⁷ have tabulated values of this integral for different strengths of the first-order Jahn-Teller coupling. In abbreviated form this matrix element is

$$g_R = g_E f_{11}, \quad (2)$$

where g_E is the electronic matrix element and f_{11} is the vibrational-overlap integral. Similarly the matrix element for the spin-orbit splitting is

$$\lambda_R = |\langle \Psi_{y,1,1/2} | \lambda L_z | \Psi_{x,1,1/2} \rangle| = \lambda_E f_{11},$$

where

$$\lambda_E = |\langle \mathcal{E}_y | \lambda L_z | \mathcal{E}_x \rangle|.$$

Figure 2(b) shows the ground state in the presence of a large strain of E symmetry which has lifted the degeneracy and split the states $\Psi_{x,1,1/2}$ and $\Psi_{y,1,1/2}$ by

¹⁷ M. S. Child and H. C. Longuet-Higgins, Phil. Trans. Roy. Soc. London 254, 259 (1961).

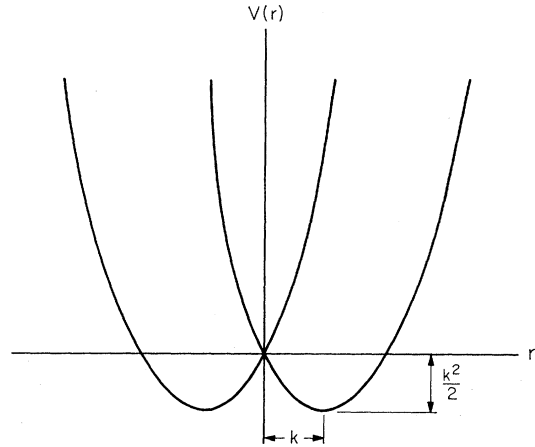


FIG. 1. An adiabatic potential-energy curve for a doubly degenerate electronic state interacting with a doubly degenerate mode of vibration. k is the first-order Jahn-Teller coupling coefficient.

energy σ . The effect of an applied magnetic field is to lift the Kramers degeneracy and produce a mixing of the states $\Psi_{x,1,1/2}$ and $\Psi_{y,1,1/2}$. For convenience in drawing Fig. 2(b), a positive spin-orbit coupling is shown only in the presence of the magnetic field.

For the R_2 transition, neglecting configuration mixing, selective absorption of left (+) or right (-) circularly polarized light can arise only from a ground-state splitting or wave-function mixing among states split by lattice distortions. In addition, there will be a difference in population of levels which preferentially absorb one sense of polarization. This effect will also give rise to a net difference in absorption. The absorption spectrum for the simplest case, the zero-phonon line, consists of two bands. Using the case shown in Fig. 2(a), the band for left (+) circular polarization arises from levels 2 and 3. That for right (-) circular polarization arises from levels 1 and 4. This is shown in Fig. 3(a). The band

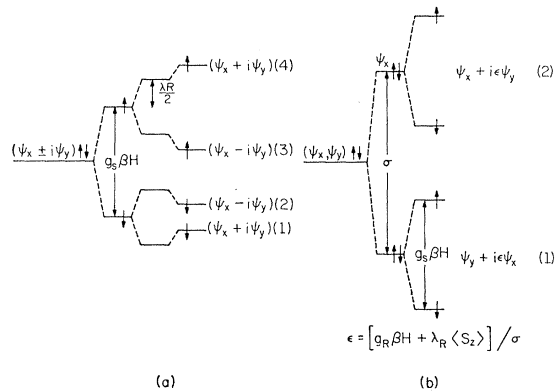


FIG. 2. R -center ground state in the presence of a magnetic field: case a —random strain equal to zero and degeneracy lifted by magnetic field; case b —orbital degeneracy lifted by random strain and strain-split levels mixed by magnetic field and spin-orbit interaction.

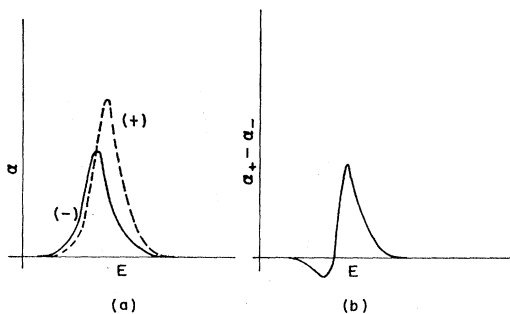
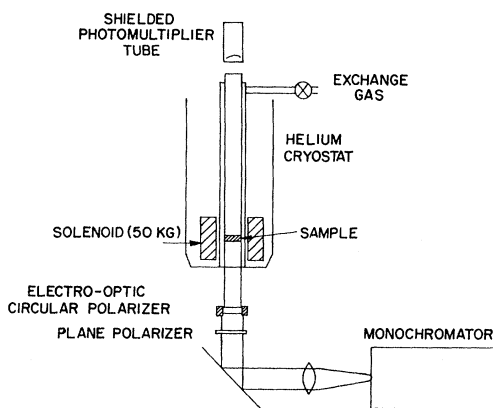


FIG. 3. (a) Absorption bands for a transition from a degenerate ground state to a singlet excited state in the presence of a magnetic field. Difference in area for left (+) and right (-) circular absorption arises from a difference in population of the absorbing energy levels. (b) Difference in absorption of two bands shown in (a).

for left circular polarization is shown as being larger due to population effects in the ground state. If the energy-level splittings are significantly smaller than the line-width because of Jahn-Teller quenching of the orbital and spin-orbit matrix elements, the separation of the bands can only be detected by measuring the difference between them. This difference spectrum for the two bands from Fig. 3(a) is shown in Fig. 3(b). From these measured changes in absorption constant the changes in the moments of the line can be calculated and related to the orbital parameters of interest by the applications of the analysis of HSS to this problem.

III. METHOD OF MEASUREMENT

The optical system used to measure the circular dichroism is shown in Fig. 4. It consists of a Bausch and Lomb 0.5-m monochromator with a 1160-line/mm grating. The sample is mounted on the end of a polished stainless-steel light-collection pipe and is positioned in the center of a 50-kG superconducting solenoid. The



SCHEMATIC DIAGRAM OF OPTICAL SYSTEM

FIG. 4. Diagram of experimental apparatus.

light passes through a fixed-sheet polarizer and a Baird-Atomic Pockels cell which serves as the circular-polarizing element. The transmitted light is then detected with a magnetically shielded photomultiplier tube. The photomultiplier high-voltage supply was regulated to maintain the photomultiplier output current constant to better than 1% during the scan of an absorption band. The electronic detection is similar to that used by Overhauser and Ruchardt.¹⁸ An ac voltage supplied by the internal oscillator of a PAR lock-in amplifier through a power amplifier and a step-up transformer is applied to the Pockels cell. For a peak voltage which produces circular-polarized light, the light in one cycle is alternately linear, right circular, linear, left circular, linear. The resultant amplitude modulation of the photomultiplier output current due to the dichroism is amplified and phase sensitively detected with the lock-in amplifier at the same frequency as the Pockels cell is driven. This system is sensitive to changes in α of less than one part in 10^4 .

An (Au+0.02 at.% Fe)-versus-Chromel-*P* thermocouple calibrated against a germanium thermometer was used to measure the temperature to an accuracy $\pm 0.15^\circ\text{K}$. No significant deviations were noted in the calibration curve in the presence of a magnetic field for the batch of wire used here. The thermocouple was glued to the sample holder. The sample was clamped to the holder by a spring loaded finger. A 0.010-in.-thick foil of indium was inserted between the sample and the holder to improve thermal contact.

The samples of KCl were cleaved from blocks supplied by Harshaw Company, colored with 100-kV x rays filtered to remove the soft x-ray component, and then bleached at room temperature with a mercury lamp to form *R* centers. Optical densities of approximately 1 for the zero-phonon line at helium temperatures were used. In the case of the zero-phonon line, optical absorption measurements were made with the sample in place in the solenoid Dewar. In the case of the *R*₁ band, absorption measurements were made at helium temperatures in a Cary 14 immediately before and after the dichroism measurement. No significant deviations in the before and after absorption curves were noted.

IV. APPLICATION OF METHOD OF MOMENTS TO DEGENERATE GROUND STATES

HSS¹⁶ defined the zeroth and first moments of an absorption band as

$$A_n = A v_a \sum_b \langle a | P_\eta^\dagger | b \rangle \langle b | P_\eta | a \rangle, \quad (4)$$

$$E_{\eta'} = A_{\eta'}^{-1} A v_a \sum_b \langle a | P_\eta^\dagger | b \rangle \langle b | P_\eta | a \rangle (E_b - E_a), \quad (5)$$

¹⁸ A. W. Overhauser and H. Ruchardt, Phys. Rev. **112**, 722 (1958).

where Av_a is a thermal average over the initial states a , \sum_b is a sum over the final states b , and P_η is the electrical dipole operator of polarization η .

The Hamiltonian and wave functions for the R -center problem can be constructed using the formalism of HSS and the results of LHOPS¹¹ and Silsbee¹ cited above. The total Hamiltonian is

$$H = H_E(\mathbf{r}) + H_L(Q) + H_{JT}(\mathbf{r}, Q) + H'(\mathbf{r}, Q, S), \quad (6)$$

where

$$H'(\mathbf{r}, Q, S) = H_{st} + H_{SO} + H_{mag}. \quad (7)$$

$H_E(\mathbf{r})$ and $H_L(Q)$ are the electronic Hamiltonian with $Q=0$ and the lattice Hamiltonian in the harmonic approximation. H_{JT} is the Hamiltonian for the linear electron-lattice interaction which for the E modes of vibration interacting with the E symmetry ground state describes the Jahn-Teller effect. The ground-state eigenfunctions for a Hamiltonian consisting of these three terms are the (Ψ_{xpl}, Ψ_{ypl}) given by Silsbee.¹

The term H_{st} is an additional electron-lattice interaction due to the presence of random strains in the crystal. H_{SO} is the spin-orbit interaction and is of the form λLS , while H_{mag} is the Hamiltonian for the applied magnetic field and has the usual form

$$H_{mag} = \beta \mathbf{H} \cdot (\mathbf{L} + 2\mathbf{S}). \quad (8)$$

In Eqs. (4) and (5) for the zeroth and first moments there is a thermal average over the ground state $|a\rangle$. The separation of the low-lying vibronic levels which are solutions for the Hamiltonian $H_E + H_L + H_{JT}$ are of the order of 80 cm^{-1} . In the temperature range below 20°K (the range of interest in this experiment) a thermal average over the ground state shows that only the lowest pair of vibronic levels $(\psi_{x,1,1/2}, \psi_{y,1,1/2})$ are populated. If we now turn on the perturbations H' , the thermal average over the ground state $|a\rangle$ is replaced by a thermal average over the set of levels arising from a splitting of the vibronic levels $(\psi_{x,1,1/2}, \psi_{y,1,1/2})$. The exact wave functions of these states are defined by

$$\langle \psi_i | 3\mathcal{C} | \psi_j \rangle = E_i \delta_{ij}. \quad (9)$$

The $|\psi_i\rangle$ and the final-state wave functions $|b\rangle$ are both product functions of vibronic and spin-wave functions. Neglecting mixing of the spin-wave functions, the complete wave functions may be written as

$$|\psi_i\rangle = |\psi_i'\rangle |m_s\rangle, \quad |b\rangle = |b'\rangle |m_s\rangle. \quad (10)$$

Rewriting Eq. (5) gives

$$\begin{aligned} \langle E_\eta' \rangle &= A_\eta^{-1} \text{Av}_{m_s} \langle m_s | \text{Av}_i \sum_j \sum_b \langle b' | P_\eta | \psi_i' \rangle \\ &\times \langle \psi_i' | E_{b'} - 3\mathcal{C} | \psi_j' \rangle \langle \psi_j' | P_\eta^\dagger | b' \rangle | m_s \rangle. \end{aligned} \quad (11)$$

The average over the initial states i reflects the difference in population of these levels. As shown in Sec. II, this difference in population is experimentally observed as a net area change of the absorption band. Subtraction

of the net area change from the observed dichroism then has the effect of equalizing the populations of the levels which absorb right circularly polarized light with those which absorb left circularly polarized light. In Eq. (11), for the first moment of an absorption band, these effects are present in the thermal average over the ground state. When the net area change is subtracted, this thermal average reduces to a sum over the states Ψ_i' . Rewriting Eq. (11) for equal populations in the ground-state levels gives

$$\begin{aligned} \langle E_\eta' \rangle &= A_\eta^{-1} \sum_{ij} \sum_{b'} \text{Av}_{m_s} \langle m_s | \langle b' | P_\eta | \psi_i' \rangle \\ &\times \langle \psi_i' | E_{b'} - 3\mathcal{C} | \psi_j' \rangle \langle \psi_j' | P_\eta^\dagger | b' \rangle | m_s \rangle. \end{aligned} \quad (12)$$

The average over spin orientation remains since the equalization of population of the orbital states does not include or imply equalization of population of the different spin orientations of the Kramers doublet associated with each orbital state. For case a of Fig. 2, this argument means that levels 1 and 2 and levels 3 and 4 can be treated as though they are equally populated. In case b , the strain split states 1 and 2 can also be treated in this manner.

The wave functions ψ_i' are defined by Eq. (9) to be the exact wave functions for the total ground-state Hamiltonian. In the absence of random strain, spin orbit, and external perturbations these wave functions are the $\psi_{k,1,1/2}$ given by Silsbee,¹ where k specifies the coordinate x or y . If mixing of vibronic levels and electronic configurations by the perturbations are neglected, then the principle of spectroscopic stability, as discussed by HSS, can be applied to this problem. We write

$$|\psi_i'\rangle = \sum_k |\psi_{k,1,1/2}\rangle \langle \psi_{k,1,1/2} | \psi_i' \rangle$$

or

$$\sum_i |\psi_i'\rangle \langle \psi_i'| = \sum_k |\psi_{k,1,1/2}\rangle \langle \psi_{k,1,1/2}|. \quad (13)$$

Substitution into Eq. (12) gives

$$\begin{aligned} \langle E_\eta' \rangle &= A_\eta^{-1} \text{Av}_{m_s} \sum_{k, k'} \sum_{b'} \langle m_s | \langle b' | P_\eta | \psi_{k,1,1/2} \rangle \\ &\times \langle k, 1, 1/2 | E_{b'} - 3\mathcal{C} | \psi_{k',1,1/2} \rangle \\ &\times \langle \psi_{k',1,1/2} | P_\eta^\dagger | b' \rangle | m_s \rangle. \end{aligned} \quad (14)$$

This expression allows one to calculate the first moment and its changes for optical transitions originating from a degenerate state in a restricted approximation. It possesses a portion of the generality of the result of HSS¹⁶ for degenerate final states, in that exact wave functions for the total Hamiltonian need not be determined. The fact that one must still contend with complicated vibronic wave functions rather than simple product functions of electronic and vibrational wave functions reflects the fact that we are dealing here with one vibrational state and not a complete set of such states. This disadvantage, however, will be compensated

for by additional information which can be obtained about the Jahn-Teller effect.

The zeroth-moment change arises in part from differences in population of the sublevels of the ground state. The thermal average cannot be replaced by a sum over these states, but must be carried out exactly. Spectroscopic stability thus can not be applied to the calculation of the zeroth-moment changes and the exact wave functions must be used. Using the low-temperature approximation that only states derived from the lowest doubly degenerate vibronic level are populated, the zeroth moment is

$$\langle A_{\eta} \rangle = A v_{m_s} A v_i \sum_{b'} \langle m_s | \langle \psi_i' | P_{\eta}^{\dagger} | b' \rangle \langle b' | P_{\eta} | \psi_i' \rangle | m_s \rangle. \tag{15}$$

Since we shall restrict our attention to individual absorption bands, mixing of different electronic configurations into the initial or final states or of higher vibronic levels into the lowest one will appear as area changes.

V. R_2 BAND Zero-Phonon Line

In this section, the changes in the first and zeroth moments for the R_2 band will be calculated and compared with the experimental results. In the first case the zero-phonon line will be analyzed. The final state of the system after this transition is a particular vibronic level. Because of this we can not make use of spectroscopic stability in writing the final-state wave function but we must use the exact vibronic wave function for this level. Since the final electronic state of the R_2

transition is of either A_1 or A_2 symmetry, Silsbee's¹ wave functions are exact and can be used (configuration mixing will be considered in the calculation of net area changes). Equation (14) can then be used to calculate the first moment of the zero-phonon line for circularly polarized light. The change in the first moment for left (+) and right (-) circularly polarized light in the presence of a magnetic field is then

$$\langle \Delta E_{\pm} \rangle = \pm A_{\pm}^{-1} |G_0|^2 \left\{ g_R \beta H - \frac{1}{2} \lambda_R \tanh \frac{g_s \beta H}{2kT} \right\}, \tag{16}$$

where g_R and λ_R were defined earlier, G_0 is the electric dipole matrix element for the zero-phonon line given by Silsbee, and g_s is the spin-g factor for the electron. The unperturbed area A_{\pm} can be calculated for either case a or b of Fig. 2 using Eq. (15). The result in both cases is the same and is

$$A_{\pm} = |G_0|^2. \tag{17}$$

Substituting into Eq. (16) gives

$$\langle \Delta E_{\pm} \rangle = \pm \left\{ g_R \beta H - \frac{1}{2} \lambda_R \tanh \frac{g_s \beta H}{2kT} \right\}. \tag{18}$$

The induced circular dichroism in the region of the R_2 band in KCl is shown in Fig. 5. The observed change in the line-shape function, which is related to the change in absorption constant by $\Delta f = C \Delta \alpha / E$, where E is the photon energy and C is a constant,¹⁶ is shown by the solid line. This effect is the sum of changes in the zeroth and higher moments of the band and an additional change which is also present at photon energies less than that of the zero-phonon line and is a monotonically

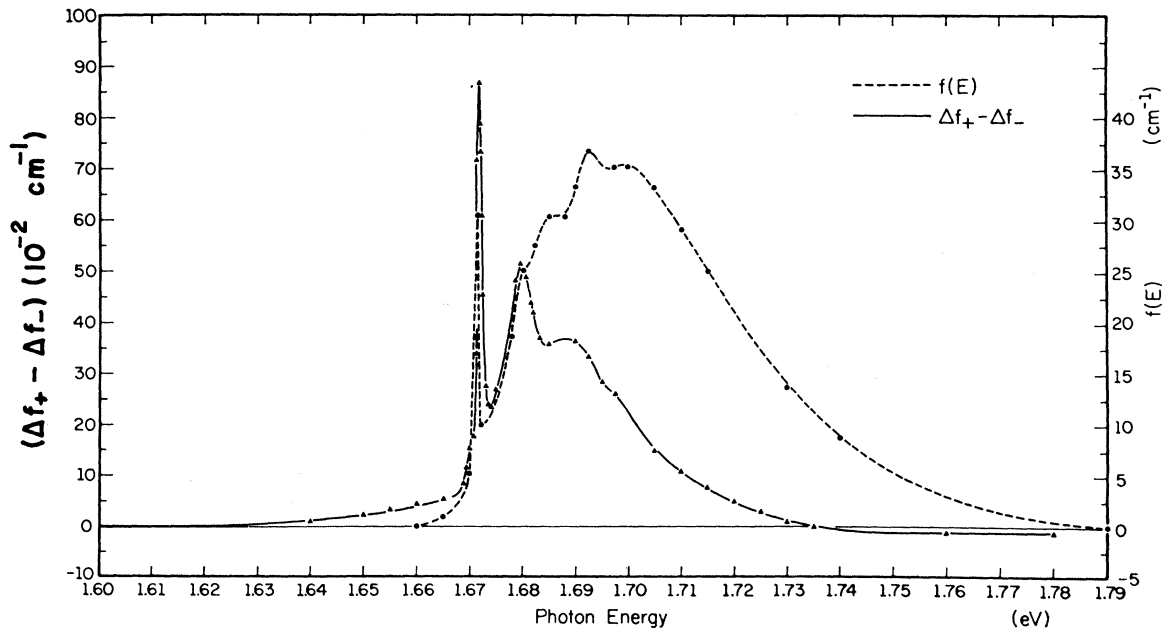


FIG. 5. Line shape (dotted line) and change in line-shape function (solid line) of the R_2 band of KCl. $H_{[001]} = 36$ kG and $T = 4.5^\circ\text{K}$.

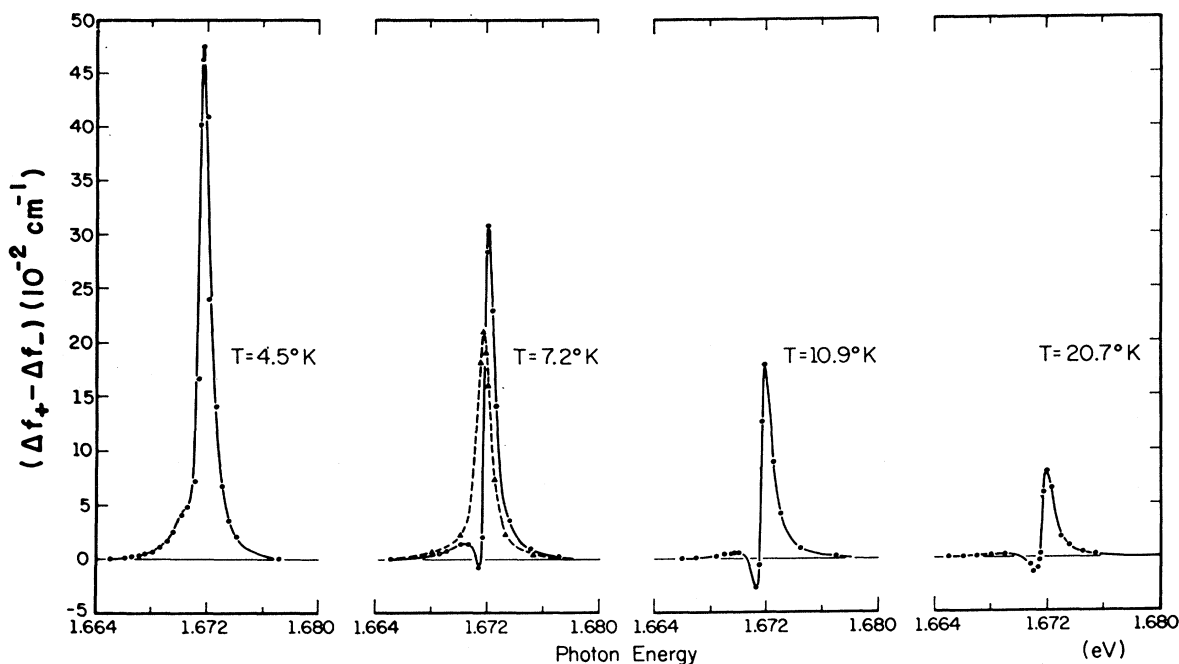


Fig. 6. Circular dichroism of the zero-phonon line of the R_2 band in KCl at $H_{[001]} = 46.6$ kG. Dotted line in 7.2°K spectra corresponds to an absorption band with the same line shape as the zero-phonon line and equal in area to the area under the measured curve (solid line). This area is the experimental zeroth-moment or area change. The difference between these two curves is used to determine the higher-moment changes.

increasing function of photon energy. This latter effect is always present in approximately the same ratio (10%) to the maximum of the zero-phonon line dichroism and decreased approximately as $1/T^2$ as the temperature was increased above 4.5°K . This temperature dependence is similar to that of the zeroth-moment change of the zero-phonon line and R_1 band which will be discussed later. These facts indicate that the effect is most likely related to the R_2 transition. However, since a noticeable change in the slope of this effect occurs at the point where the absorption due to the zero-phonon line becomes detectable, it is felt that this effect is not related to the zero-phonon line dichroism and for this reason is subtracted out.

On the high-energy side of the zero-phonon line the dichroism overlaps that due to the remainder of the R_2 band. The tail of the dichroism was extrapolated to zero at that photon energy at which the symmetrical absorption band would have an absorption constant equal to zero.

The measured line-shape change in the region of the zero-phonon line after these extrapolations is shown in Fig. 6 at different temperatures. The dashed line in the data for $T = 7.2^\circ\text{K}$ is a line-shape change which is proportional to the shape of the measured line shape of the zero-phonon line. The integrated area under this dashed curve is equal to the integrated area under the solid curve for the same temperature. This quantity is the net area or zeroth-moment change of the absorption band. The difference between these two curves is

the change in the line-shape function arising from changes in the higher moments of the line shape.

The criterion used to judge the success of the extrapolations discussed above was that the line-shape change due to the higher moments have a net area equal to zero (area of the two lobes equal), that the two lobes have the same shape, and that this shape approximate the derivative of the zero-phonon line.

The first-moment change was obtained by graphical integration of the quantity

$$\int (\delta f_+ - \delta f_-)(E - E_0) dE = A_0 (\langle \Delta E_+^1 \rangle - \langle \Delta E_-^1 \rangle),$$

where $(\delta f_+ - \delta f_-)$ is the change in line-shape function remaining after subtraction of the zeroth-moment change and E_0 is the peak position of the unperturbed absorption band. The result, plotted as a function of $1/T$ is shown in Fig. 7 and as a function of applied magnetic field in Fig. 8. It is seen that these results are in agreement with the theoretical prediction given in Eq. (18). In the high-temperature approximation using Eq. (18), $g_R = (5.5 \pm 1.5) \times 10^{-2}$ and $\lambda_R = -0.24 \pm 0.05$ cm^{-1} with $g_s = 2.03$ as determined by Krupka and Silsbee.⁵ These experimental values for g_R and λ_R include corrections for the fact that the applied field H_0 is along the $[001]$ direction ($H_{[111]} = H_0/\sqrt{3}$) and a small correction factor (0.865) due to the fact that the light propagating in the $[001]$ direction is elliptically polarized as seen in a (111) plane.

The negative sign of the spin-orbit splitting of the R -center ground state can be explained by Smith's

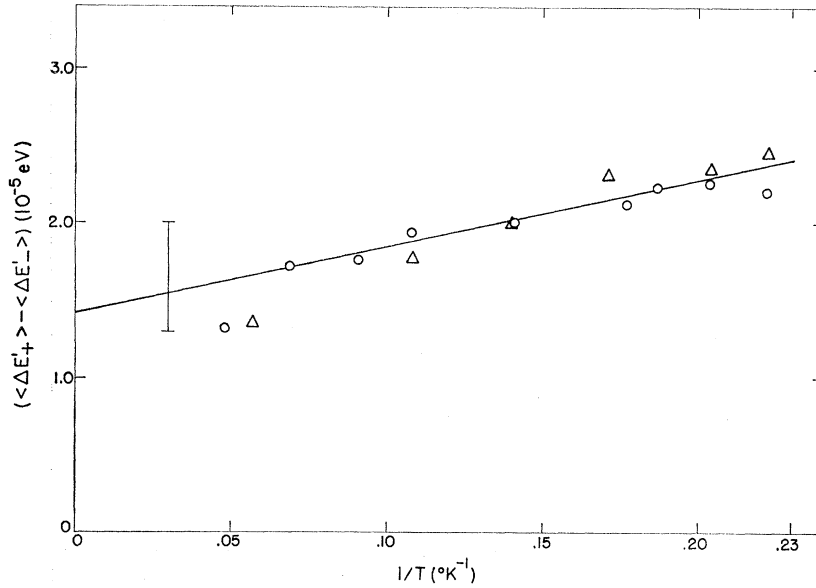


FIG. 7. First-moment change versus $1/T$ with $H_{[001]} = 46.6$ kG for the zero-phonon line of the R_2 band in KCl.

theory¹⁹ of the spin-orbit splitting of the Γ_4^- state of the F center. The orthogonalization of the R -center ground-state wave function to the core states of neighboring ions produces a spin-orbit interaction in the fields of these ions which dominates and is negative. Krupka and Silsbee⁵ have calculated the unquenched values $\lambda_E = -2.1$ cm^{-1} and $g_E = 0.48$ for the R -center ground state using this model.

From the observed spin- g shift, Krupka and Silsbee have experimentally evaluated the quantity $\lambda_E g_E$ to be equal to -5.3 cm^{-1} and the square of the first-order Jahn-Teller coupling constant to be equal to 3. In order to determine λ_E and g_E separately, Krupka and Silsbee

assumed that $(\lambda_E/g_E)_{\text{expt}} = (\lambda_E/g_E)_{\text{calc}}$ and used the experimental product $\lambda_E g_E = -5.3$ cm^{-1} to obtain

$$\lambda_E^{(\text{expt})} = -4.8 \text{ cm}^{-1}, \quad g_E^{(\text{expt})} = 1.1.$$

In this experiment the quantities λ_R and g_R were determined directly to be 0.55 and 0.24 cm^{-1} , respectively. The ratio of these experimental parameters is found to be -4.4 cm^{-1} , in good agreement with the ratio of the theoretically calculated quantities determined by Krupka and Silsbee. Using $g_E = 1.1$ and $g_R = 0.55$ the orbital reduction factor is 0.05, which corresponds to $k^2 = 3.6$.

While the errors in this experiment are large, particularly in g_R , the agreement shown above emphasizes the utility of the moments approach to the study of the effects of applied fields on degenerate initial states of optical transitions. No attempt was made in this experiment to measure changes in higher moments since these effects would emphasize the large uncertainties in the dichroism in the tails of the zero-phonon line.

The calculation of the area change of the zero-phonon line will be divided into three parts. The first part involves population effects arising from magnetic splittings within the lowest vibronic level or from wave functions mixing among strain-split states of this vibronic level. The calculation will be based upon the model shown in case b of Fig. 2 with σ as an average random-strain splitting. Keeping only those terms which are first order in magnetic field and averaging over spin, the zeroth-moment change is

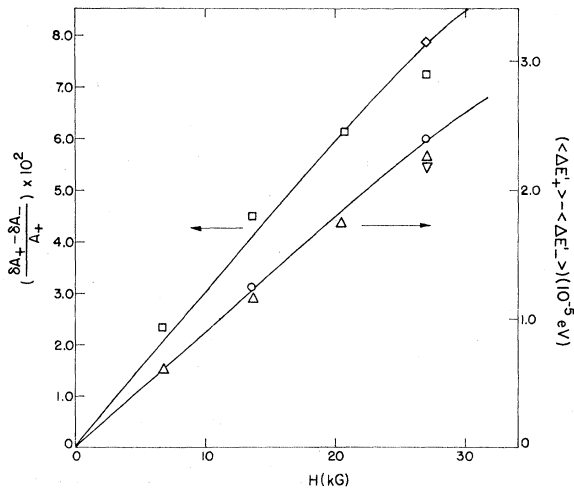


FIG. 8. Magnetic-field dependence of zeroth- and first-moment changes of the zero-phonon line of the R_2 band in KCl at $T = 4.5^{\circ}\text{K}$. H is component of the magnetic field in the $[111]$ direction.

¹⁹ D. Y. Smith, Phys. Rev. **137**, A574 (1965).

$$\frac{\delta A_{\pm}}{A_{\pm}} = \pm \frac{2}{\sigma} \left\{ g_R \beta H - \frac{1}{2} \lambda_R \tanh \frac{g_s \beta H}{2kT} \right\} \tanh \frac{\sigma}{2kT}. \quad (19)$$

Expanding $\tanh(\sigma/2kT)$ for $\sigma/2kT \ll 1$ gives

$$\frac{\delta A_{\pm}}{A_{\pm}} = \pm \frac{1}{kT} \left\{ g_R \beta H - \frac{1}{2} \lambda_R \tanh \frac{g_s \beta H}{2kT} \right\} \mp \frac{2}{3} \frac{\sigma^2}{(2kT)^3} \left\{ g_R \beta H - \frac{1}{2} \lambda_R \tanh \frac{g_s \beta H}{2kT} \right\}. \quad (20)$$

The first term is the answer which one would obtain from a calculation using the model given in case *a* of Fig. 2 ($\sigma=0$). The relative magnitude of these terms can be estimated using Silsbee's values of an average random strain of 1 kg/mm² and a splitting σ of 2.2 cm⁻¹/(kg/mm²). At 10°K

$$\left(\frac{2\sigma^2}{3(2kT)^3} \right) / \left(\frac{1}{kT} \right) \approx 0.01.$$

In the temperature range considered here (4–20°K) this term can be neglected. At 1°K or in the presence of large strains these terms will become comparable.

The applied magnetic field and the spin-orbit interaction can produce first-order wave-function changes through mixing of higher vibronic levels or other electronic configurations of *E* symmetry. These changes will be neglected since the coupling matrix elements will be of the same order as those for higher vibronic levels, but with an energy denominator which is 100 times larger. The ground-state wave functions with these perturbations become

$$|\psi_{i,1,1/2}\rangle \rightarrow |\psi_{i,1,1/2}\rangle \mp i \sum_p \epsilon_p |\psi_{i,p,1/2}\rangle, \quad (21)$$

where the subscript $i=x$ or y ,

$$\epsilon_p = |\langle \psi_{y,p,1/2} | \beta H L_z + \lambda_E L_z \langle S_z \rangle | \psi_{x,1,1/2} \rangle| / (p-1)\Delta, \quad (22)$$

and $\Delta \approx 80$ cm⁻¹ is the ground-state vibronic energy-level separation. The mixing of the *A*₁ and *A*₂ final-state configurations gives

$$|A_2 \rho_{10}\rangle \rightarrow |A_2 \rho_{10}\rangle + i \sum_n \epsilon_n |A_1 \rho_{n0}\rangle, \quad (23)$$

where

$$\epsilon_n = |\langle A_1 | \beta H L_z + \lambda L_z \langle S_z \rangle | A_2 \rangle| \sum_n \frac{\langle \rho_{n0} | \rho_{10} \rangle}{(E_0^{A_2} - E_n^{A_1})}. \quad (24)$$

Substituting Eq. (21) and Eq. (23) into Eq. (15) and neglecting ground-state population differences, the area change due to mixing is

$$\frac{\delta A_{\pm}}{A_{\pm}} = \pm 2 \left\{ \frac{g_E \beta H}{\Delta} - \frac{\lambda E}{2\Delta} \tanh \frac{g_s \beta H}{2kT} \right\} \sum_p \frac{f_p^1}{(p-1)} \frac{G_p}{G_0} \pm \left\{ g_{12} \beta H - \frac{1}{2} \lambda_{12} \tanh \frac{g_s \beta H}{2kT} \right\} \sum_n \frac{\langle \rho_{n0} | \rho_{10} \rangle}{(E_0^{A_2} - E_n^{A_1})}, \quad (25)$$

where

$$G_p = \langle A_2 \rho_{10} | x | \psi_{y,p,1/2} \rangle, \quad G_n = \langle A_1 \rho_{n0} | x | \psi_{x,1,1/2} \rangle, \\ g_{12} = \langle A_1 | L_z | A_2 \rangle, \quad \lambda_{12} = \langle A_1 | \lambda L_z | A_2 \rangle.$$

The total area change is then the sum of Eqs. (19) and (25). The measured area change of the zero-phonon line is shown as a function of the applied magnetic field in Fig. 8 and as a function of temperature by curve A in Fig. 9. The ground-state population effects can be calculated from the first-moment results and are shown as curve B of Fig. 9. The difference (A–B) is then the contribution of wave-function changes described by Eq. (25). The quantity (A–B) is of the form predicted, consisting of a “diamagnetic” and a “paramagnetic” term.

An estimate of the contribution of the ground-state term can be made in the following way. The dominant term in the matrix element G_p is the $p=2$ term and will be of order $0.1G_0$. The overlap integral f_{21} is approximately 0.07 for $k^2=3.6$ from the work of Child and Longuet-Higgins.¹⁷ For $g_E=1.1$, $\lambda_E=-4.8$ cm⁻¹, and $\Delta \approx 80$ cm⁻¹, the diamagnetic contribution is of order 0.04% and the paramagnetic contribution is 0.02% at $T=7^\circ\text{K}$. Both terms are thus negligible and the dominant contribution arises from the final-state mixing. As will be shown later, the zeroth-moment change of the *R*₁ band confirms this result.

Excited-state mixing may be investigated in the following approximation. The sum over the *A*₁ states will be replaced by some average dipole matrix element G_{A_1} and an average energy separation equal to the difference between the energy of the zero-phonon line and the peak position of the *R*_m band which Silsbee has shown arises from the transition to the *A*₁ final state.

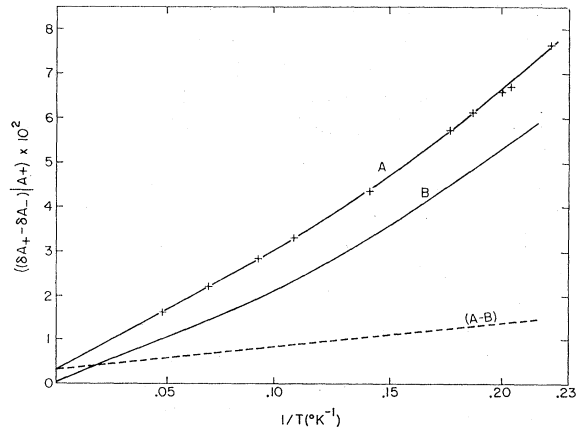


FIG. 9. Zeroth-moment change of zero-phonon line of the *R*₂ band in KCl versus $1/T$ with $H_{1001}=46.6$ kG. Curve A: experimental data; curve B: contribution of ground-state effect calculated from first-moment change using Eq. (19); curve A–B: difference between the two curves.

The ratio G_{A_1}/G_0 can then be approximated by

$$\frac{G_{A_1}}{G_0} \approx \frac{G_{A_1} G_{A_1}}{G_A G_0} = \left(\frac{A_{A_1}}{A_{A_2}}\right)^{1/2} \left(\frac{A_{A_2}}{A_0}\right)^{1/2},$$

where A_{A_1} , A_{A_2} , and A_0 are the areas of the R_m , R_2 , and zero-phonon line, respectively. Using the values $A_{A_1}/A_{A_2} \approx \frac{1}{3}$ and $A_{A_2}/A_0 \approx 50$,²⁰ $G_{A_1}/G_0 \approx 4.0$. The area change is

$$\frac{\delta A_{\pm}}{A_{\pm}} = \pm 2 \left\{ \frac{g_{12}\beta H}{\Delta_{12}} - \frac{\lambda_{12}}{2\Delta_{12}} \frac{g_s\beta H}{2kT} \right\} \{4.0\}. \quad (26)$$

Using curve (A-B) of Fig. 9,

$$g_{12} = 0.23, \quad \lambda_{12} = -6.0 \text{ cm}^{-1}.$$

These numbers serve as a crude estimate of the coupling between the A_1 and A_2 states.

Duval *et al.*¹³ estimated the magnitude of the spin-orbit splitting and orbital g factor from the measured area change of the zero-phonon line in the temperature range from 1.3 to 8°K. Their results gave a value of $g_R = 0.04$, $\lambda_R = -(1.3 \pm 0.3) \text{ cm}^{-1}$, and $k^2 \approx 3.0$. The agreement for g_R and k^2 between their measurement and the data presented above is good. Their value of the spin-orbit splitting is, however, a factor of 5 larger than that found here. A portion of this discrepancy can be explained by an error of a factor of 2 in the coefficient of their expression for the area change. Another possible source of this difference is the fact that here the background dichroism was subtracted before either the zeroth- or first-moment changes were evaluated. Duval *et al.* apparently did not perform this subtraction. There is, in addition, a zeroth-moment change due to the mixing of excited-state electronic configurations which they did not include. Any of these possible reasons for the difference in the magnitude of the spin-orbit splitting should have also produced a larger value for g_R . At this point there is no clear explanation of the discrepancies between the two measurements.

Kuwabara¹⁴ has searched for Zeeman splitting of the zero-phonon line in KCl using pulsed fields of 140 kG and unpolarized light. He found no shift or splitting of the line to within $(0.5 \pm 0.5) \text{ cm}^{-1}$. Using the value of g_R measured above, the splitting of the zero-phonon line at 140 kG would be 0.35 cm^{-1} which is within this limit. Kuwabara's result is then consistent with the results reported here.

While this paper was in preparation a prepublication report of work of Shepherd¹⁵ on the circular dichroism of the R_2 band in KCl and KF at low temperatures and low magnetic fields appeared. The analysis of the zeroth- and first-moment changes is similar to that reported above. Values of $g_R = 0.06 \pm 0.01$, $\lambda_R = -(0.32 \pm 0.03) \text{ cm}^{-1}$, and $k^2 = 3.2$ for KCl are in good agreement with

²⁰ D. B. Fitchen, R. H. Silsbee, R. A. Fulton, and E. L. Wolf, *Phys. Rev. Letters* **11**, 275 (1963).

the results presented above for high temperatures and high applied magnetic fields. By the application of a uniaxial stress Shepherd also showed that the dependence of the zeroth-moment change on strain splitting is in agreement with Eq. (19). No estimate was made of the spin-orbit and magnetic-field mixing of the A_1 and A_2 symmetry excited states.

R_2 Broad-Band Dichroism

The broad-band dichroism of the R_2 band in KCl is shown in Fig. 5. This spectrum is qualitatively different from that associated with the zero-phonon line. These differences can be explained from a calculation of the zeroth- and first-moment changes for the broad band using the same approximation on the ground state as those used for the zero-phonon line.

Since we are dealing with an orbital singlet in the final state we can write the states as product functions of electronic and lattice wave functions. The area of the R_2 band is then

$$A_{\pm} = A v_{m_s} A v_i \sum_l \langle m_s | \langle \psi_i | P_{\eta}^{\dagger} | A_2 \rangle | X_l \rangle \times \langle X_l | \langle A_2 | P_{\eta} | \psi_i \rangle | m_s \rangle, \quad (27)$$

where X_l are the complete set of E - and A_1 -mode vibrational states for the R -center problem. A further simplification of Eq. (27) by invoking completeness can not in general be made since the sign of the vibrational-overlap integral between the initial and final states depends upon whether the initial state is $\psi_{x,1,1/2}$ or $\psi_{y,1,1/2}$. This effect is important only in those terms where a mixing of $\psi_{x,1,1/2}$ and $\psi_{y,1,1/2}$ are present. To calculate this overlap in detail we can use the excited-state wave functions given by Silsbee¹ with $m=0$ and $m=1$ since they constitute the only members of the complete set of E -mode vibrational states which have a nonzero overlap with the ground states.

Substituting into Eq. (27) and carrying out the integration over angles, the zeroth-moment change due to the ground-state population distribution is

$$\frac{\delta A_{\pm}}{A_{\pm}} = \pm \frac{4}{\sigma} \left\{ g_R \beta H - \frac{1}{2} \lambda_R \tanh \frac{g_s \beta H}{2kT} \right\} \times \tanh \left(\frac{\sigma}{2kT} \right) \left\{ \frac{\sum_n |A_{n0}|^2 - \sum_n |B_{n1}|^2}{\sum_n |A_{n0}|^2 + \sum_n |B_{n1}|^2} \right\}, \quad (28)$$

where

$$A_{n0} = \int r dr \rho_{n0} [u_{1,1/2}(-r) + u_{1,1/2}(+r)],$$

$$B_{n1} = \int r dr \rho_{n1} [u_{1,1/2}(-r) - u_{1,1/2}(+r)],$$

and all other quantities are defined as in the case of the zero-phonon line. The overlap integrals A_{n0} and B_{n1} are those for the E modes. The A -mode overlap integrals

cancel between numerator and denominator. Mixing of the A_1 and A_2 configurations is neglected since we will only consider the qualitative aspects of the dichroism.

The first-moment change for the R_2 band can also be calculated in this framework using Eq. (11) and is

$$\langle \Delta E_{\pm} \rangle = \pm \left\{ g_R \beta H - \frac{1}{2} \lambda_R \tanh \frac{g_0 \beta H}{2kT} \right\} \times \left\{ \frac{\sum_n |A_{n0}|^2 - \sum_n |B_{n1}|^2}{\sum_n |A_{n0}|^2 + \sum_n |B_{n1}|^2} \right\}. \quad (29)$$

These results show that the sign of the moment changes depends upon the final vibrational state and is opposite in sign for states corresponding to the excitation of an even or odd number of E -mode vibrational quanta. This effect may be understood physically if one refers back to the model calculation of LHOPS.¹¹ The quantum number which characterizes the rotational motion of the coupled electron-nuclear system in the Jahn-Teller regime is $l = m + \frac{1}{2}j$, where m is the vibrational angular quantum number and j is a quantum number which characterizes the rotational motion of the electron. For the lowest vibrational level of the ground states $l = \frac{1}{2}$, two combinations of m and j are possible:

$$m=0 \quad j=1 \quad \text{and} \quad m=1 \quad j=-1,$$

the significance of the sign of j being to indicate the sense of rotation of the electron. Since $\Delta m = 0$ in the optical transition, the sense of the electronic rotation in the ground state is opposite in sign for the transitions to final vibrational levels with $m=0$ and $m=1$. This opposite sense of rotation in the ground state will then produce the observed difference in sign in the induced dichroism.

The sign of the dichroism is insensitive to the excitation of A -mode vibrational quanta. The A -mode excitations can then be considered as sidebands on the E -mode spectra, with the sign of the dichroism depending only upon the number of E -mode quanta excited.

With these facts in mind we can now consider Fig. 5 again and draw several conclusions. The first sideband of the zero-phonon line at 1.680 eV is seen as a peak in $f(E)$ and is a positive peak in the dichroic spectra. It can thus be identified as the first A_1 -mode sideband of the zero-phonon line. The energy of an A_1 -mode quanta is then 8.0 meV. The peak at 1.685 eV in $f(E)$ and the corresponding depression in the dichroic spectra at this energy indicates that this peak corresponds to the first E -mode sideband of the zero-phonon line. The energy of an E -mode quanta is then approximately 13.0 meV. Table I contains a listing of several sidebands of the R_2 zero-phonon line in KCl, LiF, and NaCl for which symmetry assignments can be made in this way. The data for LiF are shown in Fig. 10 and those for NaCl in Fig. 11. In Fig. 10 the R_2 line-shape function at 77°K

TABLE I. Assignments of the symmetry of lattice excitations associated with vibronic sidebands of the zero-phonon line and the phonon branch and propagation direction corresponding to the excitation.

Photon energy of the sideband (eV)	Lattice excitation energy (meV)	Symmetry assignment	Phonon assignment
KCl			
1.680	8	A_1	$A_1 = \text{TA}_{(100)}$
1.685	13	E	
1.688	16	$2 \times A_1$	$E = \text{TO}_{(111)}$
1.6925	20.5	$E + A_1$	
1.6970	25	$3 \times A_1$	
		$2 \times E$	
LiF			
3.200	28	A_1	$A_1 = \text{TO}_{(111)}$
3.240	68	E	$E = \text{LO}_{(100)}$
NaCl			
1.974	14	A_1	$A_1 = \text{TA}_{(111)}$
1.978	18	E	
1.985	25	$2 \times A_1$	$E = \text{LA}_{(100)}$

is shown. This is sufficient for our needs since the energies of the peaks in the line shape do not shift significantly below 77°K in LiF. The theoretical phonon energies obtained by Pierce²¹ from the dispersion curves of Karo and Hardy²²⁻²⁴ were used to make the assignments of particular branches and propagation directions for the lattice excitations.

These results are in agreement with Pierce's finding that the coupling is primarily to lattice phonons. The phonon assignments presented here differ in several places from those of Pierce. The reason for this lies in that here the assignments depend more upon the number of phonons excited than upon agreement with the theoretical phonon energies. An example of this is the vibronic sideband of the zero-phonon line in LiF which appears at approximately 3.240 eV. The circular dichroism pattern indicates that this sideband is associated with the excitation of an odd number of E -mode quanta and most probably one such quantum. The phonon assignment must then be that for a single phonon rather than the two-phonon assignment given by Pierce.

The symmetry assignments for the first two sidebands in KCl are in agreement with those of Duval *et al.*¹³ from a circular-dichroism measurement and the estimate of Silsbee¹ from the stress dichroism. The result that the dichroism in KCl goes to zero at 1.735 eV and then changes sign, is also in agreement with the work of Silsbee, who showed that the $m=0$ and $m=1$ spectra become equal at approximately this energy. Shepherd¹⁵ has made a similar analysis of the dichroism of the zero-phonon-line sideband spectra in KF and identified the

²¹ C. B. Pierce, Phys. Rev. **135**, A83 (1964).

²² A. M. Karo and J. R. Hardy, Phys. Rev. **129**, 2024 (1963).

²³ J. R. Hardy and A. M. Karo, Phil. Mag. **5**, 859 (1960).

²⁴ J. R. Hardy, Phil. Mag. **7**, 315 (1962).

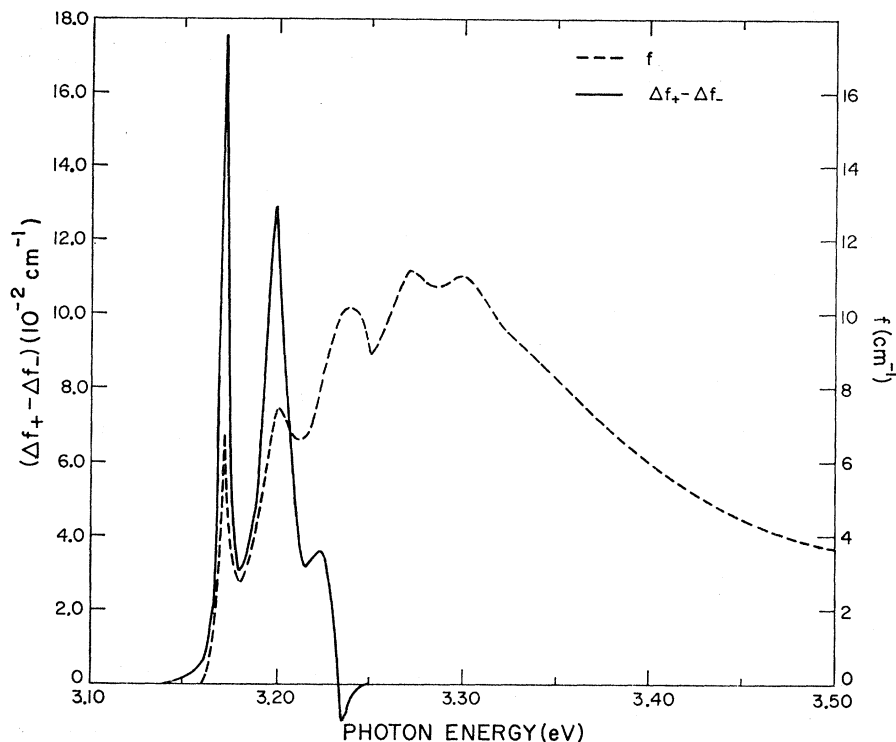


FIG. 10. Line shape (dotted line) and change in line-shape function (solid line) of the R_2 band in LiF. $T=4.5^\circ\text{K}$ and $H_{[100]}=36\text{ kG}$. $f(E)$ was measured at 77°K .

number of E -mode phonons associated with a particular sideband.

VI. R_1 BAND

The R_1 band has been shown by Silsbee¹ to be an E -to- E transition of the R center. The band is broadened by the interaction of the excited state with distortions of both A and E symmetry. Since we are dealing with degeneracies in both the initial and final states, the

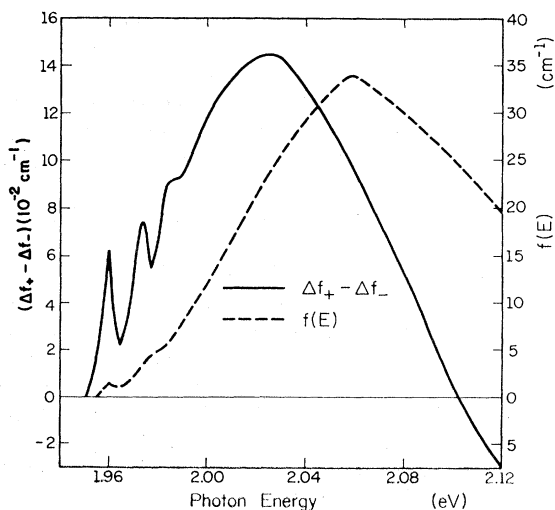


FIG. 11. Line shape (dotted line) and change in line-shape function (solid line) of the R_2 band in NaCl. $T=4.5^\circ\text{K}$ and $H_{[100]}=46.6\text{ kG}$.

measured shift of the absorption band for circularly polarized light will be the difference between the excited- and ground-state splittings. The measured circular dichroism in the region of the T_1 band is shown in Fig. 12. These data show an area change opposite in sign to that for the R_2 band and a "derivative" type pattern indicative of a magnetic splitting. These results can be quantitatively analyzed using the approximations and results of the previous sections on the zero-phonon line and R_2 broad-band dichroism.

The calculation of the excited-state effects follows the formalism of HSS. The final-state wave functions $|b\rangle$ are defined by

$$\langle b|\mathcal{H}|b'\rangle = E_b\delta_{bb'}. \quad (30)$$

Using the principle of spectroscopic stability these wave functions may be written

$$\sum_b |b\rangle\langle b| = \sum_e \sum_l \sum_m |eX_l m\rangle\langle eX_l m|.$$

The first moment can then be written as

$$\begin{aligned} \langle E_\eta' \rangle &= A_\eta^{-1} A V_{m_s} \\ &\times \sum_k \sum_e \sum_l \langle m_s | \langle \psi_{k,1,1/2} | P_\eta^\dagger | eX_l \rangle (E_b - E_k) \\ &\times \langle eX_l | P_\eta | \psi_{k,1,1/2} \rangle | m_s \rangle. \end{aligned} \quad (31)$$

This expression must then be broken up into two parts since both the initial and final states are perturbed by the applied magnetic field.

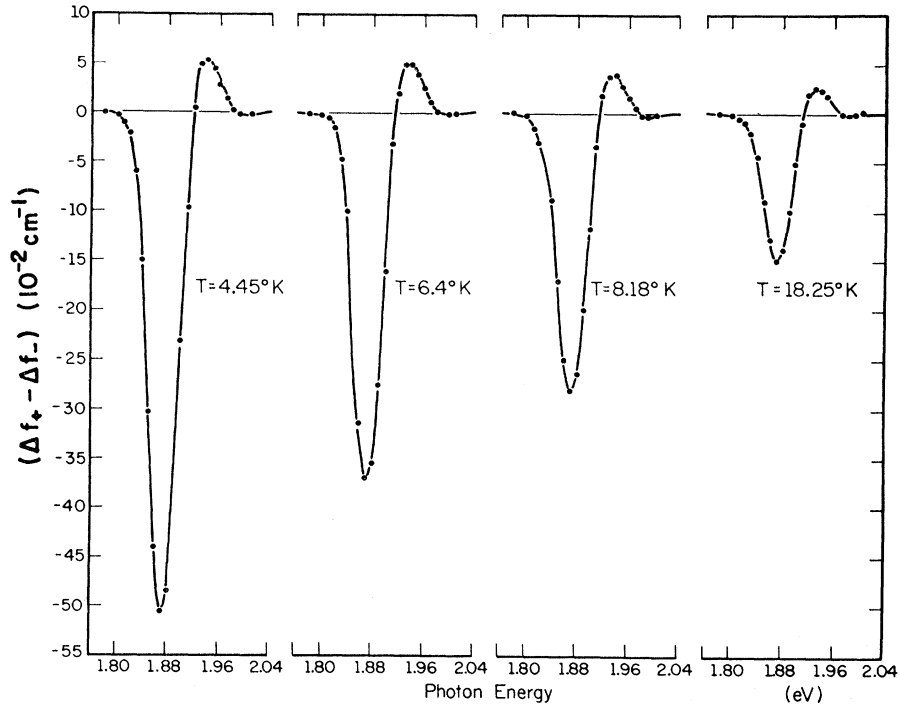


FIG. 12. R_1 -band circular dichroism in KCl for $H_{(001)} = 46.6$ kG at several temperatures.

Since the sign of the dipole matrix element depends upon whether the initial state is $\psi_{x,1,1/2}$ or $\psi_{y,1,1/2}$, the explicit vibrational wave functions must be used in the calculation of the ground-state effect. To first order, the calculation of the excited-state effect is diagonal in the ground-state wave function so that for this term the completeness relation $\sum_i |X_i\rangle\langle X_i| = 1$ can be used.

The final-state electronic wave functions are linear combinations of the “ p ”-like wave functions of the unperturbed F centers. The signs of the perturbing matrix elements and the electric-dipole matrix elements from the ground state (0) to the final state (1) depend upon which linear combinations are chosen. If these combinations are chosen such that $\langle \mathcal{E}_y^1 | L_z | \mathcal{E}_x^1 \rangle = g_1$ is positive, then the electric-dipole matrix elements are $\langle \mathcal{E}_x^1 | x | \mathcal{E}_x^0 \rangle = \langle \mathcal{E}_y^1 | y | \mathcal{E}_x^0 \rangle = \langle \mathcal{E}_y^1 | x | \mathcal{E}_y^0 \rangle = -\langle \mathcal{E}_x^1 | y | \mathcal{E}_y^0 \rangle$ which differ in sign in the first and last elements from those of Silsbee.¹ With these definitions and the spin-orbit matrix element $\langle \mathcal{E}_y^1 | \lambda L_z | \mathcal{E}_x^1 \rangle = \lambda_1$ the first-moment change for circularly polarized light is

$$\begin{aligned} \langle \Delta E_{\pm}' \rangle = & \pm \left\{ g_1 \beta H - \frac{1}{2} \lambda_1 \tanh \frac{g_s \beta H}{2kT} \right\} \\ & \mp \left\{ g_R \beta H - \frac{1}{2} \lambda_R \tanh \frac{g_s \beta H}{2kT} \right\} \\ & \times \frac{\left\{ \sum_n |A_{n0}|^2 - \sum_n |B_{n1}|^2 \right\}}{\left\{ \sum_n |A_{n0}|^2 + \sum_n |B_{n1}|^2 \right\}}. \quad (32) \end{aligned}$$

The zeroth-moment change of the R_1 band is

$$\begin{aligned} \frac{\delta A_{\pm}}{A_{\pm}} = & \mp \frac{2}{\sigma} \left\{ g_R H - \frac{1}{2} \lambda_R \tanh \frac{g_s \beta H}{2kT} \right\} \tanh \frac{\sigma}{2kT} \\ & \times \frac{\sum_n |A_{n0}|^2 - \sum_n |B_{n1}|^2}{\sum_n |A_{n0}|^2 + \sum_n |B_{n1}|^2}, \quad (33) \end{aligned}$$

which predicts the observed change in sign of the zeroth moment from the case of the R_2 band. Zeroth-moment changes due to mixing of excited-state configurations or mixing of higher vibronic levels of the ground state are not presented since they are not necessary for the discussion of the results.

In the analysis of the data for the R_1 band, the M_4 band observed by Okamoto²⁵ and Rabin²⁶ was subtracted to obtain the area of the unperturbed R_1 band.

The observed zeroth-moment change, plotted as a function of $1/T$, is shown in Fig. 13. The dotted line in this figure is a theoretical curve calculated from Eq. (33) for

$$\frac{\sigma}{2kT} \ll 1, \quad \frac{\sum_n |A_{n0}|^2 - \sum_n |B_{n1}|^2}{\sum_n |A_{n0}|^2 + \sum_n |B_{n1}|^2} = \frac{1}{2}.$$

The good fit to the data in the high-temperature range indicates that this estimate for the difference factor is a good one. The difference between the two curves in Fig. 13 could be due to either mixing of excited-state

²⁵ F. Okamoto, Phys. Rev. **124**, 1090 (1961).

²⁶ H. Rabin, Phys. Rev. **129**, 129 (1963).

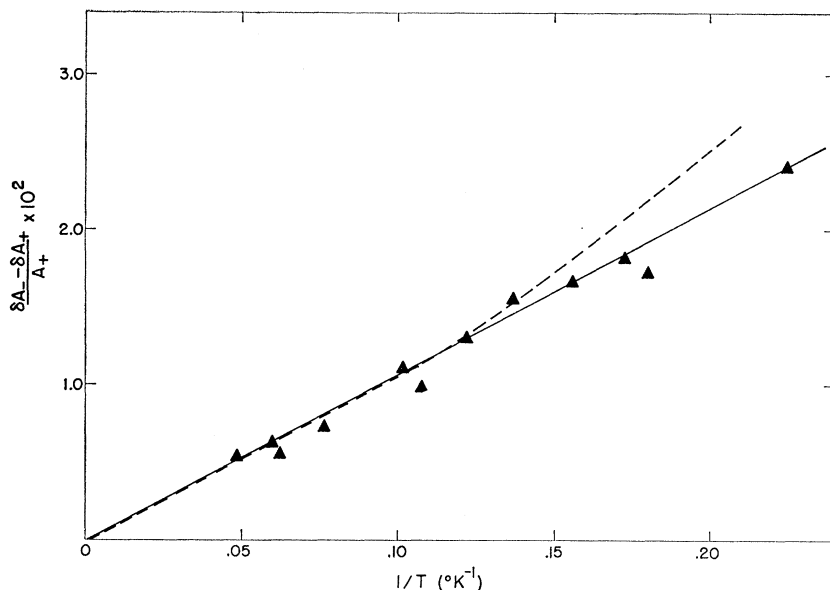


FIG. 13. Zeroth-moment change of R_1 band in KCl with $H_{[001]}=46.6$ kG. Dotted curve calculated from Eq. (33).

configurations or higher-order terms in the random strain becoming important. Both of these terms are of the correct sign to explain this effect. The difference occurs over such a small temperature range and is of such a size that any definite interpretation would be questionable. There is no significant temperature-independent term at high temperatures as would be the case if mixing of higher vibronic levels of the ground state into the lowest level were important. This is in agreement with the estimate made in the discussion of the zeroth-moment change of the zero-phonon line.

The field dependence of both the first- and the zeroth-moment change are shown in Fig. 14. The results indicate that the effects are first order in the magnetic field in agreement with Eqs. (32) and (33).

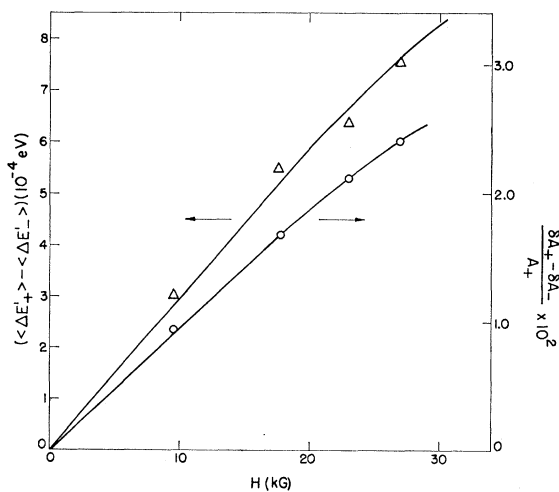


FIG. 14. Field dependence of zeroth- and first-moment changes of R_1 band in KCl at $T=4.5^\circ\text{K}$. H is the component of magnetic field in the $[111]$ direction.

The temperature dependence of the first-moment change of the R_1 band is shown in Fig. 15. Using the approximate value of $\frac{1}{2}$ for the difference factor and applying the corrections for the field direction and degree of circular polarization discussed earlier, the data give $g_1=0.40\pm 0.1$ and $\lambda_1=-15\pm 2$ cm^{-1} . The actual value of the difference factor is not crucial since the ground-state term contributes less than 5% to the value of the first-moment change.

From the zeroth-moment change of the zero-phonon line an estimate of the coupling of the A_1 and A_2 final states was obtained. These values were $g_{12}\approx 0.23$ and $\lambda_{12}\approx -6$ cm^{-1} which do not differ significantly from the corresponding values for the final state of the R_1 band. This agreement is not unreasonable since all of these states are in a first approximation linear combinations of the Γ_4^- states of the F centers which combine to form the R center.

The results of the circular-dichroism measurement on the R_1 band can be consistently interpreted on the basis of an E -symmetry final state for the R_1 transition and with the estimate of a small dynamic Jahn-Teller effect in the excited state.¹ The experimentally observed circular dichroism would be qualitatively quite different if the Jahn-Teller effect were large with the second component of the doublet lying under the F band. In the region of the R_1 band, there would be an additional area change due to mixing of the two components such as was seen by Henry²⁷ for the F_A center.

VII. CONCLUSIONS

The circular dichroism of the R_2 and R_1 transitions of the R center has been measured and analyzed using the method of moments of HSS. The analysis used here was

²⁷ C. H. Henry, Phys. Rev. **140**, A256 (1965).

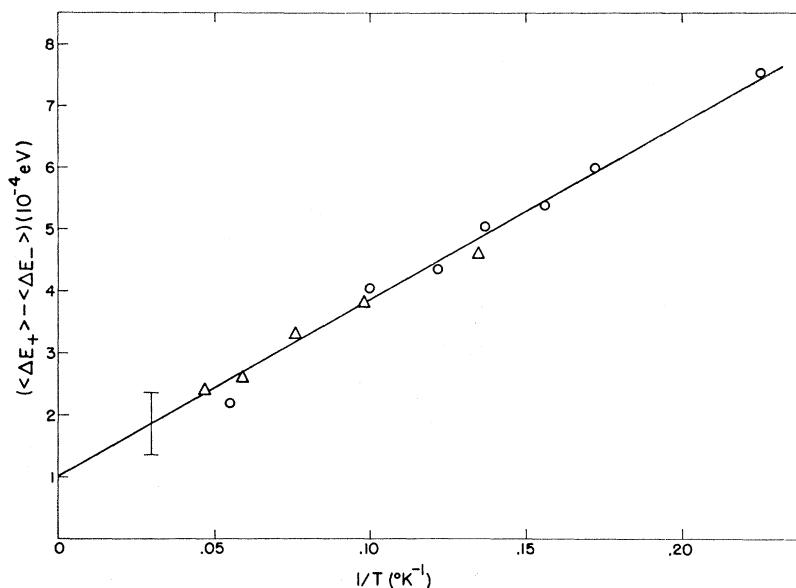


FIG. 15. First-moment changes of R_1 band in KCl versus $1/T$ with $H_{[001]} = 46.6$ kG.

not as general as that of HSS due to the fact that ground-state degeneracy is involved. These restrictions, however, provided additional information concerning the electron-lattice interaction in the ground state. For both transitions the zeroth- and first-moment changes were analyzed. Higher-moment changes were not analyzed since the overlap of adjacent bands and large zeroth-moment changes would make their determination quite inaccurate. For both the R_2 and R_1 transitions the data could be consistently interpreted using the symmetry assignments given for the electronic states by Silsbee.

From the first-moment change of the zero-phonon line an orbital g factor equal to 0.055 ± 0.015 , a spin-orbit splitting equal to $-(0.24 \pm 0.05) \text{ cm}^{-1}$, and a value of the square of the first-order Jahn-Teller coupling constant k^2 equal to 3.6 were obtained for the R -center ground state in KCl. Good agreement with the results of Krupka and Silsbee and Shepherd was found. The zeroth-moment change was found to be due to differences in population of ground-state levels and configuration mixing of the A_1 and A_2 final states. The magnitude of the orbital and spin-orbit mixing of these states was estimated after the ground-state effect was subtracted.

The broad-band dichroism of the R_2 band exhibited cancellation effects arising from Jahn-Teller mixing of ground-state vibrational levels. This mixing produced opposite signs for the circular dichroism of vibrational sidebands which involve the excitations of an odd or

even number of E -symmetry phonons. The effect was used to determine the symmetry of phonons associated with several of the vibrational sidebands of the zero-phonon line in KCl, LiF, and NaCl.

An orbital g factor equal to 0.4 ± 0.1 and a spin-orbit splitting equal to $-(15 \pm 2) \text{ cm}^{-1}$ of the E -symmetry final state of the R_1 transition in KCl were also measured. The spin-orbit splitting of this state and the ground state were negative as in the case of the F center. The zeroth-moment change of this transition was almost completely due to the ground-state population distribution. Comparison of the zeroth-moment changes for both the zero-phonon line and the R_1 transition showed that mixing of higher vibronic levels of the ground state into the lowest vibronic level was not important.

ACKNOWLEDGMENTS

The author wishes to express his appreciation to Professor W. D. Compton for his advice and help during this work. The author also wishes to thank Dr. S. E. Schnatterly, who participated in the preliminary measurements of these effects, and with whom the author had many informative discussions. Numerous helpful discussions with Professor C. P. Slichter, Professor Horst Seidel, Dr. E. L. Wolf, and R. E. Hetrick are also acknowledged. The technical assistance provided by D. O. Skaperdas is appreciated.